Chiral symmetry restoration and the Z_3 sectors of QCD

Christof Gattringer, P. E. L. Rakow, Andreas Schäfer, and Wolfgang Söldner
Institut für Theoretische Physik, Universität Regensburg, D-93040 Regensburg, Germany
(Received 13 February 2002; published 13 September 2002)

Quenched QCD has a Z_3 phase transition which is explicitly broken for dynamical calculations. Knowing whether or not the chiral phase transition occurs at the same temperature for all Z_3 sectors and whether this critical temperature coincides with the deconfinement transition could be crucial to understand the underlying microscopic dynamics also for the full theory. We use the existence of a gap in the Dirac spectrum as an order parameter for the restoration of chiral symmetry. We find that the spectral gap opens up at the same critical temperature in all Z_3 sectors in contrast with earlier claims in the literature.

DOI: 10.1103/PhysRevD.66.054502 PACS number(s): 12.38.Gc, 11.15.Ha, 11.30.Rd

One of the most widely discussed puzzles of QCD is the relationship between the deconfinement and chiral phase transition. In the quenched approximation the Polyakov loop is an order parameter and the theory has a Z_3 [1] symmetry the spontaneous breaking of which defines the deconfinement phase transition with a critical temperature T_{Z_3}. For vanishing quark mass the chiral condensate $\langle \overline{\psi}\psi \rangle$ is an order parameter for chiral symmetry breaking which vanishes above a critical temperature T_χ. In the real world quark masses are nonzero and the center symmetry Z_3 is explicitly broken. In this case one can define some deconfinement temperature T_{dec} from the analysis of e.g. the energy density or the heavy quark-antiquark potential. There is much debate about the underlying mechanisms which link these different transition temperatures (see e.g. [2]) which can be summarized by the following question: "Are T_{Z_3}, T_χ and T_{dec} related and, if yes, how precisely?" This can probably only be answered by identifying the relevant microscopic dynamics. In [3] it was claimed that the restoration of chiral symmetry happens at different temperatures in the real ($\varphi \sim 0$) and complex sectors of the Polyakov loop ($\varphi \sim \pm 2\pi/3$) which, if true, suggests that there is at least no simple relationship between T_{Z_3} and T_χ. Obviously the question of whether this observation is correct is thus highly important for this whole discussion. Reference [3] inspired various attempts [4] to find possible mechanisms to explain a higher transition temperature for the complex sector or even a complete absence of chiral symmetry restoration for the case of SU(2) configurations with negative Polyakov loop. Also, there exists a large literature more generally related to this question; see [5,6] for some examples. Let us note that even if it were irrelevant for full QCD the center symmetry could still lead to fascinating phenomenological consequences in supersymmetric Yang-Mills theories [5]. Thus the investigation of its properties is also relevant on more general grounds.

In this paper we reexamine this problem within lattice QCD using chirally improved fermions. In contrast to [3], which used staggered fermions, we find that the critical β of the chiral phase transition does not depend on the Z_3 sector, but is coincident with the Z_3 breaking transition in all three sectors.

Instead of directly measuring the chiral condensate we analyze in detail the spectrum of the lattice Dirac operator. The density $\rho(\lambda)$ of the eigenvalues λ of the Dirac operator is connected to the chiral condensate via the Banks-Casher formula [7],

$$\langle \overline{\psi}\psi \rangle = -\frac{\pi}{V}\rho(0), \tag{1}$$

where $\rho(0)$ is the eigenvalue density near the origin and V is the volume of the box. Note that exact zero modes which come from isolated instantons do not contribute to the density $\rho(0)$ at the origin. The reason is that the number of zero modes is believed to scale as $V^{1/2}$ and thus they do not contribute when performing the thermodynamic limit in Eq. (1). At low temperatures when QCD is in the chirally broken phase the density is nonzero at the origin, while in the high temperature phase ρ is zero in a finite region around the origin, i.e. the spectrum develops a gap (up to isolated zero modes) and the chiral condensate vanishes (compare Fig. 1 below). The question of whether chiral symmetry is restored at the same critical temperature in all sectors of the Polyakov

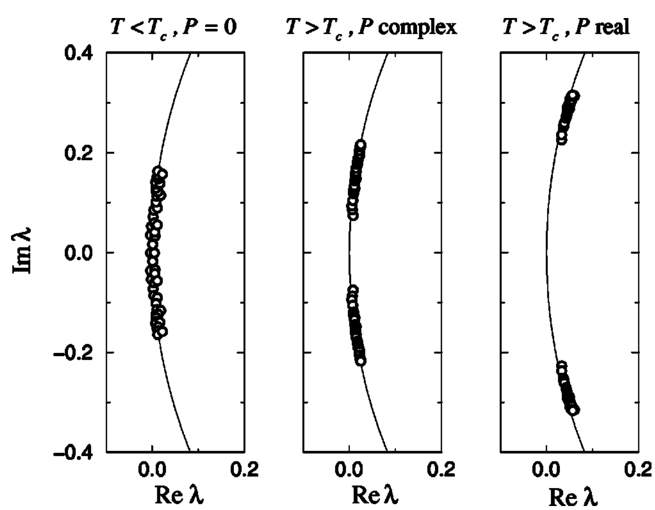

FIG. 1. Three typical spectra of the chirally improved operator. Only the 50 eigenvalues closest to the origin are plotted. Left plot: the chirally broken phase ($6\times 20^3, \beta = 8.10$); central plot: the symmetric phase ($6\times 20^3, \beta = 8.60$) for complex Polyakov loop; right plot: the symmetric phase for real Polyakov loop. The full curve is the Ginsparg-Wilson circle.

TABLE I. Parameters for our gauge field configurations. We list the values of β, the lattice spacing a and the temperature T.

β	8.10	8.20	8.25	8.30	8.45	8.60
a(fm)	0.125	0.115	0.110	0.106	0.094	0.084
T(MeV)	264	287	299	311	350	391

loop can now be reformulated in terms of the spectral gap: As we increase the temperature, does the gap open up at the same temperature for all three sectors of the Polyakov loop?

Before the advent of chirally symmetric formulations for the lattice Dirac operator such a study was quite awkward. In particular the spectrum of the Wilson lattice Dirac operator shows large fluctuations close to the origin [8] and the notion of a spectral density is not well defined. The situation has changed, since the rediscovery of the Ginsparg-Wilson equation [9]. Dirac operators D which obey the Ginsparg-Wilson equation have eigenvalues which lie on a circle and it is straightforward to identify a spectral density and study the emergence of the spectral gap. However, the only exact solution of the Ginsparg-Wilson equation, the overlap operator [10], has the drawback of being very expensive in a numerical implementation.

Here we work with the *chirally improved operator* which is a systematic expansion of a solution of the Ginsparg-Wilson equation [11]. In particular we use an approximation which has 19 terms in the expansion and is described in detail in [12,13]. The computation of the eigenvalues of the Dirac operator was done with the implicitly restarted Arnoldi method [14].

For our quenched gauge configurations we use the Lüscher-Weisz action [15]. We work on lattices of size $L_T \times L^3$ with the temporal extent $L_T=6$ and two values for the spatial extent, $L=16$ and $L=20$. We use periodic boundary conditions for the gauge fields, while for the fermions the boundary conditions are periodic only for the space directions but antiperiodic for the time direction. Our statistics is 800 configurations for the 6×16^3 lattices and 400 for the 6×20^3 lattices. We use 6 different values of the inverse coupling β which gives rise to ensembles on both sides of the phase transition. In Table I we list our values of β, the lattice spacing a [16] and the temperature T. We used the coefficients given by tadpole-improved perturbation theory [15,17]. Our values for the couplings β_{rt} and β_{pg} for the rectangle and parallelogram terms in the Lüscher-Weisz action can be found in [16].

The division of the configurations into subsets with real and complex Polyakov loop is implemented as follows: Configurations which have a Polyakov loop with a phase $|\varphi| \leq 2\pi/6$ are assigned to the real sector while all other configurations fall in the complex sector. For the high temperature phase this allows for a clear separation of the three sectors of the Polyakov loop even on a finite lattice as can e.g. be seen from the scatter plots for the Polyakov loops shown in [13].

Let us begin the discussion of the spectral gap with a look at typical spectra of our Dirac operator. In Fig. 1 we show the distribution in the complex plane of the 50 smallest eigenvalues λ for three different gauge configurations on 6×20^3 lattices. The symbols are our numerical results and the full curve is the so-called Ginsparg-Wilson circle, i.e. the circle of radius 1 in the complex plane with center 1. For our approximate Ginsparg-Wilson operator the eigenvalues do not fall exactly on the circle but show small fluctuations around the circle. However, the eigenvalues are sufficiently well ordered to allow for the notion of a spectral density and a clear identification of the spectral gap.

The plot on the left-hand side shows the spectrum for a configuration in the low temperature, chirally broken phase. For this case the eigenvalues extend all the way to the origin and there is a nonvanishing $\rho(0)$ such that the Banks-Casher relation (1) gives rise to a nonvanishing chiral condensate.

The central and the right-hand side plots show spectra for configurations in the high-temperature, chirally symmetric phase. The central plot is for a configuration with complex Polyakov loop P, while the right-hand side result is for real Polyakov loop. Both of these plots have a well pronounced spectral gap. The spectral density at the origin vanishes and so does the chiral condensate. For the complex sector the gap is considerably smaller than for the real sector.

One can understand this difference between the sectors by considering the fermion boundary conditions. In the real sector the boundary condition

$$\psi(\vec{x},t+1/T)=-\psi(\vec{x},t) \tag{2}$$

gives a Matsubara frequency πT to the fermions. In the complex Z_3 sectors the boundary condition is effectively

$$\psi(\vec{x},t+1/T)=e^{\pm i\pi/3}\psi(\vec{x},t), \tag{3}$$

giving a Matsubara frequency $\pi T/3$. In the free-field case (i.e. $\beta\to\infty$) the smallest eigenvalue is equal to the Matsubara frequency, giving a gap 3 times larger in the case of Eq. (2) compared with Eq. (3). It is thus reasonable that the real sector gap is considerably larger than the complex sector gap in the interacting case too.

In quenched QCD the finite temperature phase transition appears to be a weak first order phase transition [18]. A first order phase transition is governed by the mixing of two phases and the behavior of their free energies. In our particular example we have a low temperature phase characterized by a vanishing spectral gap and a high temperature phase with a finite spectral gap. For temperatures sufficiently below or above the critical temperature the system is in only one of the two phases while near the critical temperature the system shows mixing of the two phases.

We demonstrate this mixing in Fig. 2 where we show histograms for the distribution of the spectral gap at three different values of the temperature. We define the spectral gap g_λ to be the imaginary part of the smallest eigenvalue which is not a topological zero-mode (as remarked above, these modes do not contribute to the spectral density). Topological modes can be identified uniquely since for our chirally improved operator it can be shown that they have exactly vanishing imaginary part and the corresponding

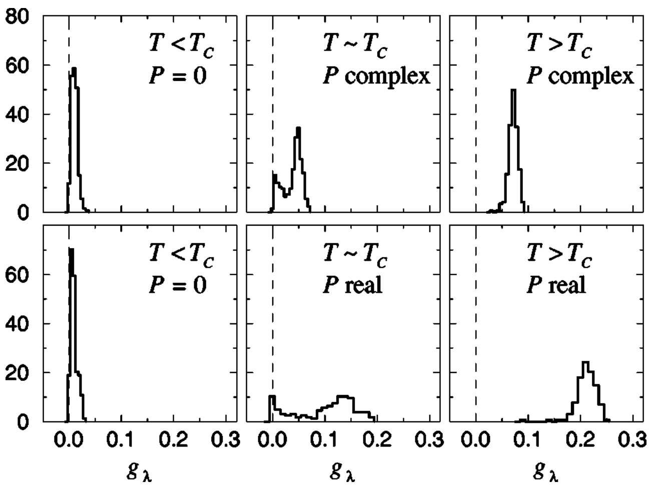

FIG. 2. Histograms for the spectral gap ag_λ. We show our results for lattice size 6×20^3 at three temperatures $T<T_c(\beta=8.10), T\sim T_c(\beta=8.30)$ and $T>T_c(\beta=8.60)$. The top row displays the results for the complex sector of the Polyakov loop P, while the bottom row is for real Polyakov loop.

eigenstates have a nonvanishing matrix element with γ_5, while this matrix element vanishes identically for nonzero modes.

We show histograms for the distribution of g_λ for $T<T_c, T\sim T_c$ and for $T>T_c$. The top row displays the results for the complex sector of the Polyakov loop P, while the bottom row is for real Polyakov loop. The data were computed on 6×20^3 lattices. Since for the real sector ($\varphi\sim 0$) the statistics is only half of the statistics for the complex sector ($\varphi\sim +2\pi/3$ and $-2\pi/3$) we doubled the bin size for the two histograms in the real sector at $T\sim T_c$ and $T>T_c$.

At $T<T_c$ we find for all sectors a single peak near the origin. This peak is not located exactly at 0 since also in the chirally broken phase the Dirac operator of a finite system has a microscopical gap which vanishes as L^{-3} [19]. For temperatures near T_c the histograms show a clear double peak structure characteristic for the first order transition. The left peak corresponds to the chirally broken phase with a vanishing gap and the right peak is from the chirally symmetric phase with nonvanishing gap. As one increases the temperature further, only the right peak survives. As already noted in the discussion of Fig. 1 the gap is larger in the real sector, i.e. the right peak sits at larger values of g_λ for the real sector. In addition this peak is wider than the corresponding peak in the complex sector, i.e. the gap fluctuates more strongly around its mean value in the real sector.

In order to describe the first order transition we use a simple ansatz for the behavior of observables. Let us first discuss the somewhat simpler case of the Polyakov loop. In an infinite system the Polyakov loop P vanishes below β_c and has a nonvanishing modulus $|P|$ above β_c. On a finite lattice the Polyakov loop does not vanish exactly below β_c but disappears like $V^{-1/2}$, i.e. like $cL^{-3/2}$ with some constant c. Above β_c the dependence on L is negligible and to leading order $|P|$ is linear in β, i.e. described by $d+k(\beta-\beta_c)$. Fol-

TABLE II. Values of β_c and the critical temperature from the analysis of the Polyakov loop and the spectral gap in the complex and the real sectors for the ensembles with Lüscher-Weisz action and chirally improved fermions.

Measurement :	$\langle\|P\|\rangle$	$\langle g_\lambda\rangle_{complex}$	$\langle g_\lambda\rangle_{real}$
β_c:	8.24(1)	8.29(2)	8.27(2)
T_c(MeV):	296(3)	308(5)	303(5)

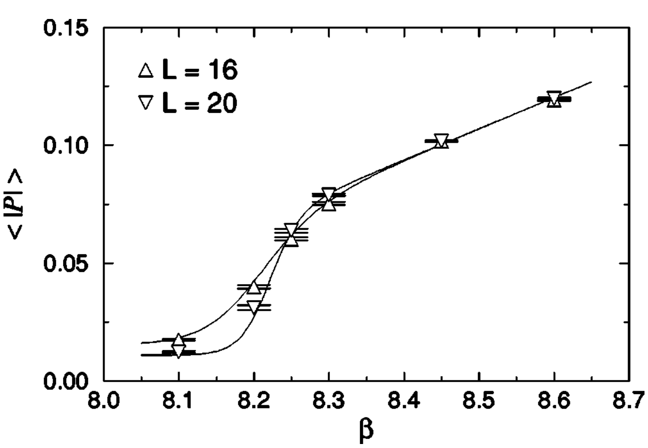

FIG. 3. The expectation value $\langle|P|\rangle$ of the modulus of the Polyakov loop as a function of β. The symbols indicate the numerical results while the curve is a fit to Eq. (4). We display results for 6×16^3 and 6×20^3 lattices.

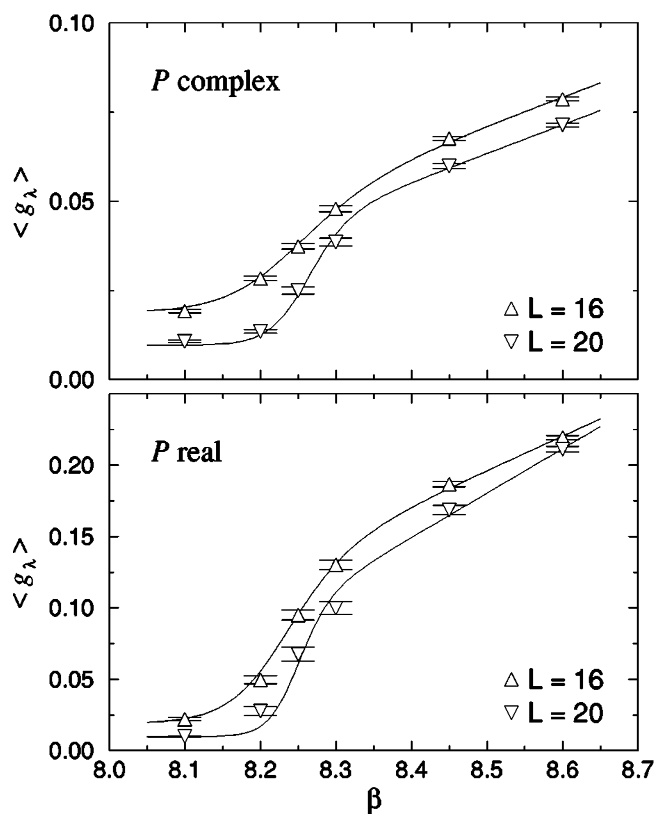

FIG. 4. The spectral gap in lattice units as a function of β. The symbols indicate the numerical results and the full curve is a fit to formula (5). We display results for 6×16^3 and 6×20^3.

lowing the ideas in [20] one arrives at the conclusion that near the transition the expectation value of $|P|$ should be given by

$$\langle |P| \rangle = \frac{cL^{-3/2} e^{-\Delta f L^3 (\beta-\beta_c)} + 3[d + k(\beta-\beta_c)]}{e^{-\Delta f L^3(\beta-\beta_c)} + 3}. \tag{4}$$

The term $-\Delta f V(\beta-\beta_c)$ is the difference in the free energies of the two phases. At $\beta=\beta_c$ the two free energies are equal while below β_c the free energy of the chirally broken phase is smaller than the free energy of the chirally symmetric phase and vice versa above β_c. The factors 3 in the second terms in the numerator and denominator come from the three possible values for the phase of the Polyakov loop. In Fig. 3 we show a fit of Eq. (4) (curves) to our numerical data (symbols). In particular we present a common fit to both the 6×16^3 and 6×20^3 ensembles. This is possible since the parameters d and k are essentially independent of L. The fit result for β_c is given in Table II below. The fit shows that both the L and the β dependence are well described by Eq. (4). We use a similar ansatz for the spectral gap g_λ:

$$\langle g_\lambda \rangle_{r,c} = \frac{c' L^{-3} e^{-\Delta f L^3(\beta-\beta_c)} + 3[d_{r,c}(L) + k_{r,c}(L)(\beta-\beta_c)]}{e^{-\Delta f L^3(\beta-\beta_c)} + 3}. \tag{5}$$

The subscripts r and c indicate the real and complex sectors of the Polyakov loop respectively. Note that now we use the known L^{-3} behavior of the microscopical spectral gap in the chirally broken phase [19]. In the chirally symmetric phase the gap is essentially linear in β but the coefficients $d_{r,c}$ and $k_{r,c}$ turn out to be L dependent. Thus in a common fit to the 6×16^3 and 6×20^3 ensembles these parameters had to be varied independently. Again the fit results for β_c are given in Table II. In Fig. 4 we plot our numerical data for the gap together with the curves (5). The top plot gives the results for the complex sector while the bottom plot shows the real sector. As for the Polyakov loop we find that the numerical data are reasonably well described by the simple first order transition formula. When comparing the results for the critical beta as given in Table II we find that within the accuracy we achieved the spectral gap vanishes at the same β_c for both the real and the complex sectors of the Polyakov loop. Furthermore this value is compatible with β_c as obtained from the analysis of the Polyakov loop. Combining the three methods we find a critical temperature of 300 ± 3 MeV for the Lüscher-Weisz action which is slightly larger than the result for Wilson's gauge action.

The numerical calculations were done on the Hitachi SR8000 of the Leibniz Rechenzentrum in Munich. We thank the staff of the LRZ for training and support. C.G. acknowledges support by the Austrian Academy of Sciences (APART 654).

[1] A.M. Polyakov, Phys. Lett. **72B**, 477 (1978); B. Svetitsky and L.G. Yaffe, Nucl. Phys. B: Field Theory Stat. Syst. **B210** [FS6], 423 (1982).
[2] H. Satz, Fortschr. Phys. **50**, 541 (2002); F. Karsch, hep-lat/0106019.
[3] S. Chandrasekharan and N.H. Christ, Nucl. Phys. B (Proc. Suppl.) **47**, 527 (1996).
[4] P.N. Meisinger and M.C. Ogilvie, Phys. Lett. B **379**, 163 (1996); S. Chandrasekharan and S. Huang, Phys. Rev. D **53**, 5100 (1996); M.A. Stephanov, Phys. Lett. B **375**, 249 (1996).
[5] A. Campos, K. Holland, and U.J. Wiese, Phys. Rev. Lett. **81**, 2420 (1998); K. Holland and U.J. Wiese, in ''At the Frontier of Particle Physics,'' edited by M. Shifman, Vol. 3, hep-ph/0011193.
[6] C. Bernard *et al.*, Phys. Rev. Lett. **78**, 598 (1997); P.H. Damgaard *et al.*, Phys. Lett. B **440**, 129 (1998); F. Lenz and M. Thies, Ann. Phys. (N.Y.) **268**, 308 (1998); C. Alexandrou *et al.*, Phys. Rev. D **60**, 034504 (1999); J.M. Verbaarschot and T. Wettig, Annu. Rev. Nucl. Part. Sci. **50**, 343 (2000).
[7] T. Banks and A. Casher, Nucl. Phys. **B169**, 103 (1980).
[8] C. Gattringer and I. Hip, Nucl. Phys. **B541**, 305 (1999); **B536**, 363 (1998).
[9] P.H. Ginsparg and K.G. Wilson, Phys. Rev. D **25**, 2649 (1982).
[10] R. Narayanan and H. Neuberger, Phys. Lett. B **302**, 62 (1993); Nucl. Phys. **B443**, 305 (1995).
[11] C. Gattringer, Phys. Rev. D **63**, 114501 (2001).
[12] C. Gattringer, I. Hip, and C.B. Lang, Nucl. Phys. **B597**, 451 (2001).
[13] C. Gattringer, M. Göckeler, P.E.L. Rakow, S. Schaefer, and A. Schäfer, Nucl. Phys. **B618**, 205 (2001).
[14] D.C. Sorensen, SIAM J. Matrix Anal. Appl. **13**, 357 (1992); R. B. Lehoucq, D.C. Sorensen, and C. Yang, *ARPACK User's Guide* (SIAM, New York, 1998).
[15] M. Lüscher and P. Weisz, Commun. Math. Phys. **97**, 59 (1985); **98**, 433(E) (1985); G. Curci, P. Menotti, and G. Paffuti, Phys. Lett. **130B**, 205 (1983); **135B**, 516(E) (1984).
[16] C. Gattringer, R. Hoffmann, and S. Schaefer, Phys. Rev. D **65**, 094503 (2002).
[17] M. Alford, W. Dimm, G.P. Lepage, G. Hockney, and P.B. Mackenzie, Phys. Lett. B **361**, 87 (1995); G.P. Lepage and P.B. Mackenzie, Phys. Rev. D **48**, 2250 (1993); J. Snippe, Nucl. Phys. **B498**, 347 (1997).
[18] G. Boyd *et al.*, Nucl. Phys. **B469**, 419 (1996).
[19] J.J.M. Verbaarschot and T. Wettig, Annu. Rev. Nucl. Part. Sci. **50**, 343 (2000).
[20] C. Borgs and R. Kotecký, Phys. Rev. Lett. **68**, 1734 (1992); C. Borgs and W. Jahnke, *ibid.* **68**, 1738 (1992).